Reassessing GRB high-energy emission correlations using a large, homogeneous sample of X-ray afterglows

Alessandro Armando Vigliano[1,2]
Francesco Longo[1,2]
Zeljka Bosnjak[3]

23 July 2026,
Sexten – Dolomites Italy

[1]University of Trieste, Trieste, Italy
[2]Istituto Nazionale di Fisica Nucleare (INFN), sezione di Trieste, Trieste, Italy
[3]University of Zagreb, Zagreb, Croatia

Do high-energy GRBs have simpler X-ray afterglows?

doi: 10.1051/0004-6361/202558494

Can X-ray morphology predict high-energy GRBs?

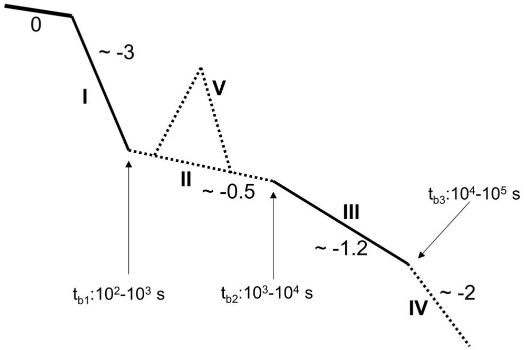

"Canonical" X-ray afterglow
0 prompt
I steep decay
II plateau/shallow decay
III normal decay
IV post jet break
V flares

Zhang et al. ApJ 2006

Previous claim: HE/VHE-detected GRBs more often show single-power-law X-ray afterglows
Yamazaki et al. 2020

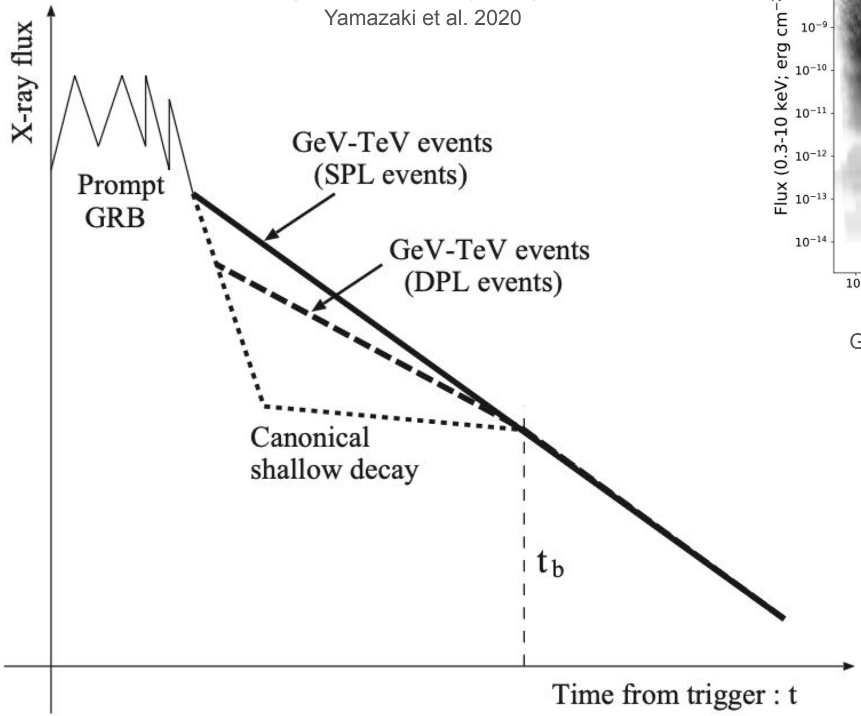

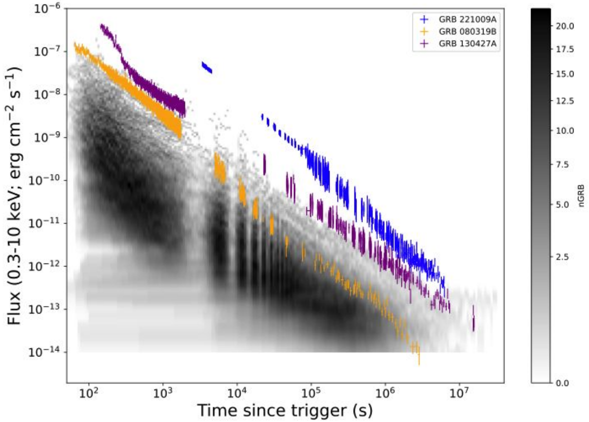

GRB 221009A vs. the Swift-XRT population
Williams et al. 2023

1438 afterglows analyzed, 1215 enter the HE comparison

Complete Swift-XRT catalogue

- **• 1438 light curves pass the initial selection**
- **• uniform flare removal and segmented fitting**

HE test sample (post-2008)

- 92 HE/VHE detections
- 1123 without HE detection
- only 7 VHE events

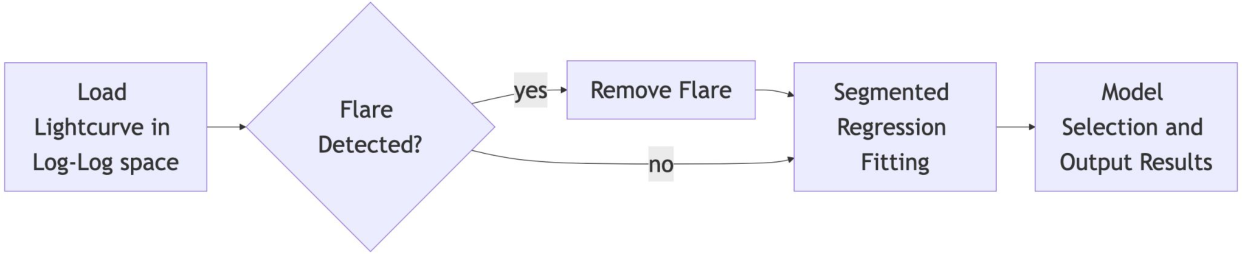

Uniform analysis reduces analyst-dependent choices, but it does not remove observational selection.

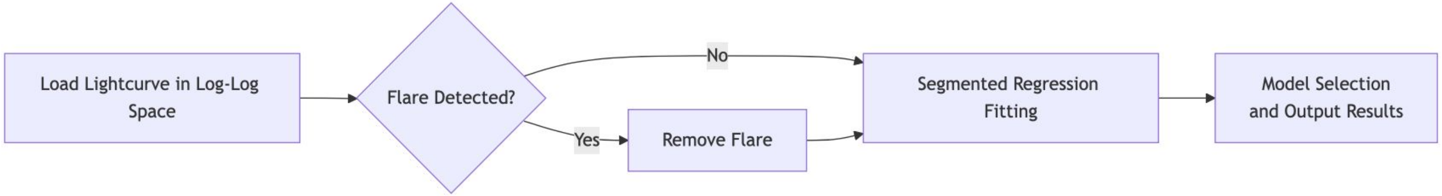

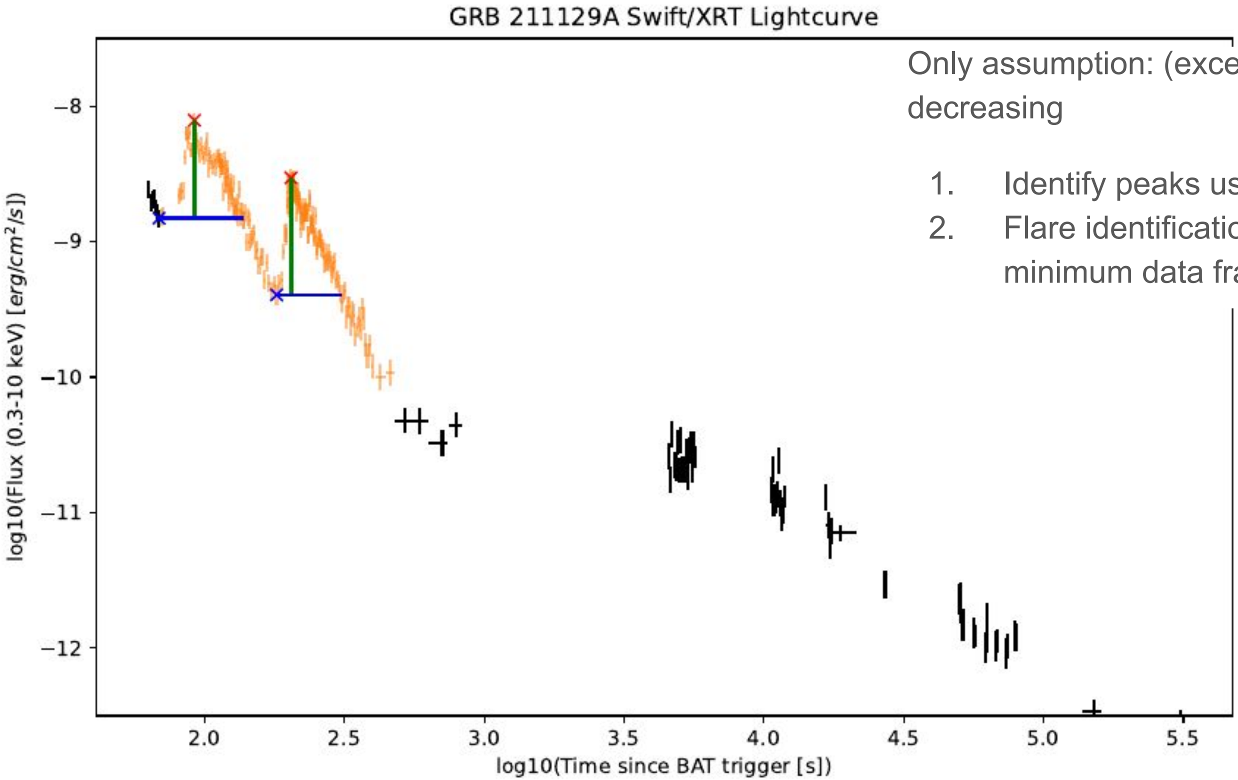

Only assumption: (except for flares) the lightcurve is generally decreasing

1. Identify peaks using their prominence and width
2. Flare identification: minimum significance of the peak and minimum data fraction in the rising part

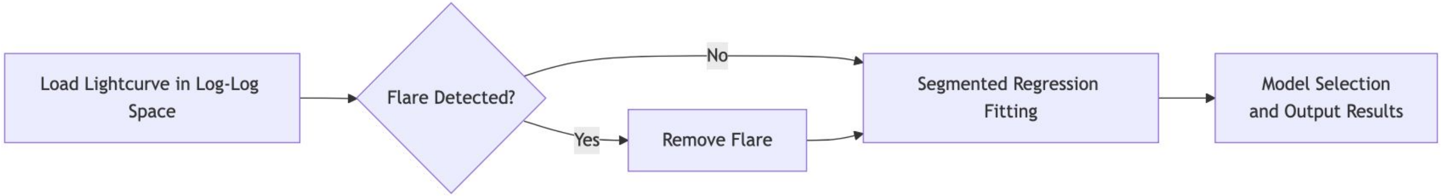

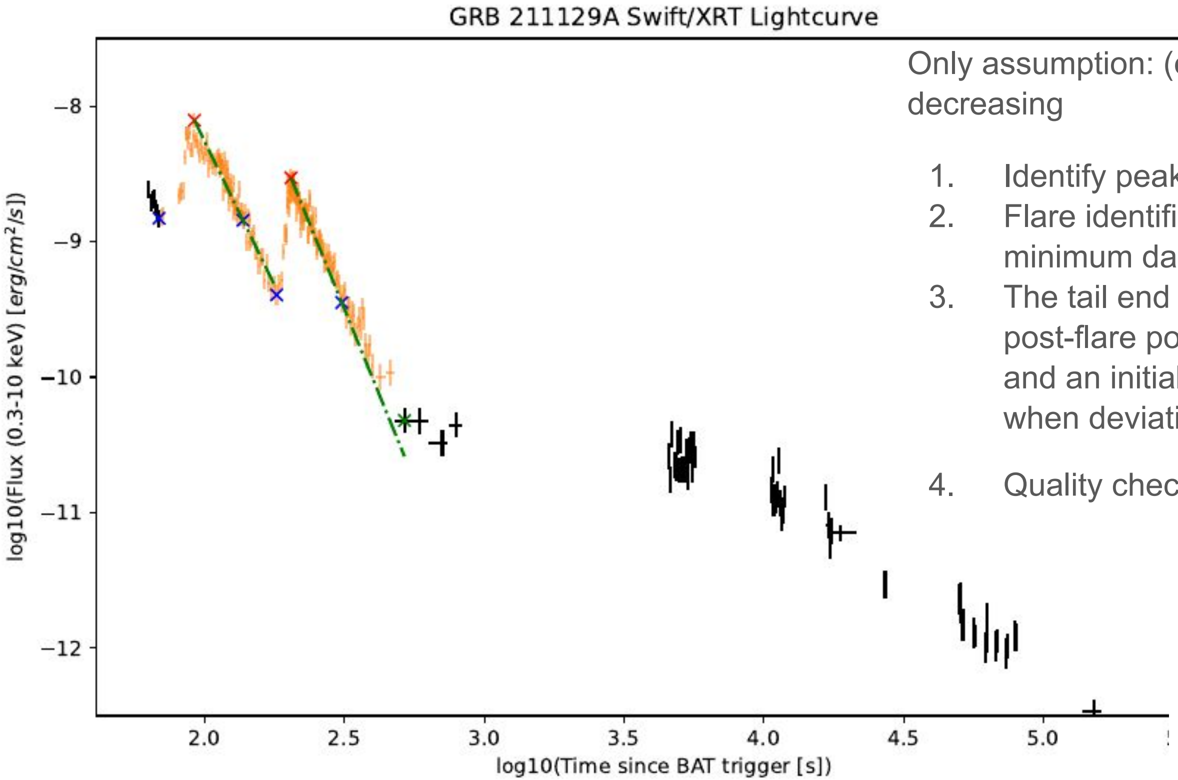

Only assumption: (except for flares) the lightcurve is generally decreasing

1. Identify peaks using their prominence and width
2. Flare identification: minimum significance of the peak and minimum data fraction in the rising part
3. The tail end of each flare is determined by comparing post-flare points to a reference slope between the peak and an initial parallel point. The flare is considered ended when deviations exceed a threshold
4. Quality checks: e.g. outlier detection

Identifies at least a flare in approx 29.6% (426/1438) of the GRBs in the Swift-XRT Catalog, in line with the values generally found in the literature (≈30% Liu & Mao 2019)

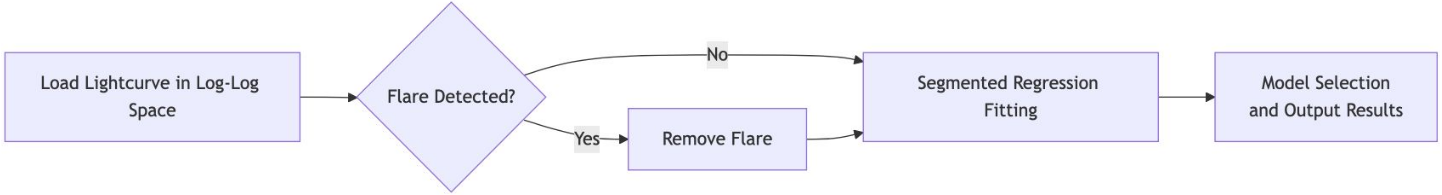

Log-Log space → segmented regression → Muggeo's method (Muggeo, Wiley 2003, DOI: 10.1002/sim.1545)

$$y = c + \alpha_1 x + \sum_{k=1}^{N} \beta_k (x - \psi_k) H(x - \psi_k)$$

E.g.: for a single breakpoint:

$$y = \alpha x + c + \beta(x - \psi) H(x - \psi)$$

Taylor expansion around an estimate of the breakpoint to linearize the dependance on phi and repeat the fit iteratively:

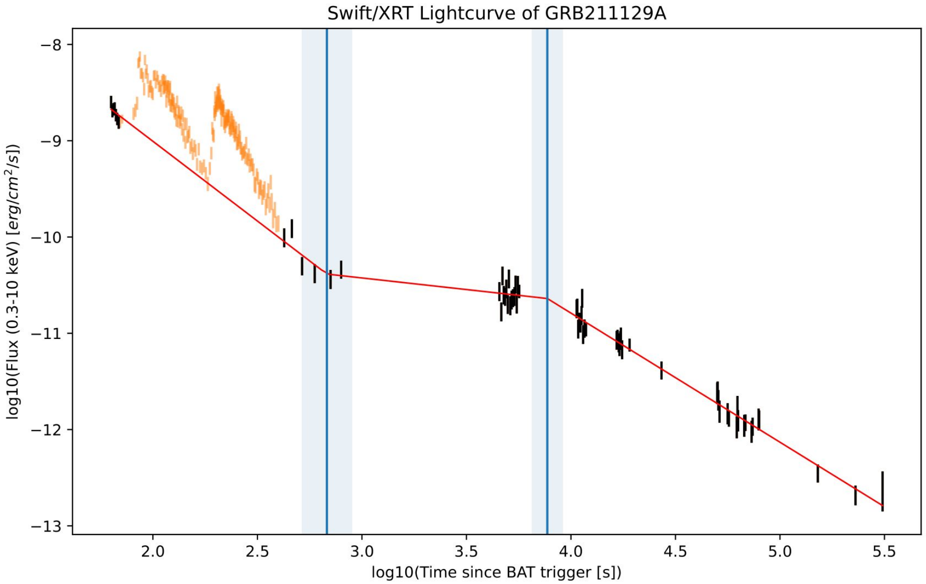

$$y \approx \alpha x + c + \beta(x - \psi^{(0)}) H(x - \psi^{(0)}) - \beta(\psi - \psi^{(0)}) H(x - \psi^{(0)})$$

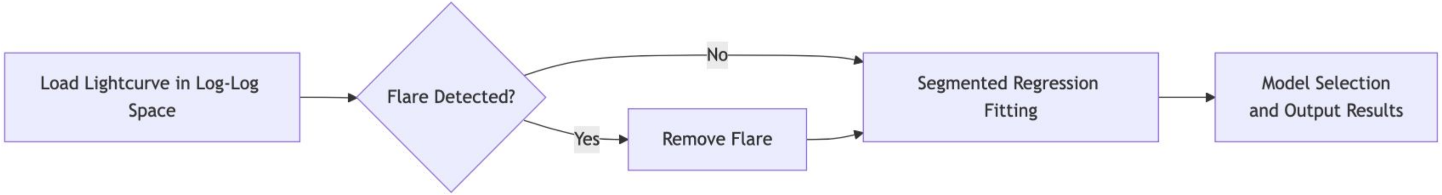

- Need to compare all the models for selecting the best fit → BIC
- Few datapoints? → need flexibility to choose the best statistics:

$$\mathrm{BIC} := -2\log(L) + k\log(n),$$

$$\mathrm{AICc} := -2\log(L) + \frac{2k(k+1)}{n-k-1},$$

$$\mathrm{BICc} := -2\log(L) + \frac{n}{n-k-2}k\log(n),$$

$$\mathrm{EvBIC} := -2\left(1-\frac{1}{n}\right)\log(L) + k\log(n),$$

$$\begin{cases} n = \text{number of points} \\ k = \text{number of free parameters} = 2(1+N_{breaks}) \end{cases}$$

McQuarrie, S&PL (1999), https://doi.org/10.1016/S0167-7152(98)00294-6
Bickel, SP (2025), https://doi.org/10.1007/s00362-025-01682-1

Two morphological observables: breaks and plateaus

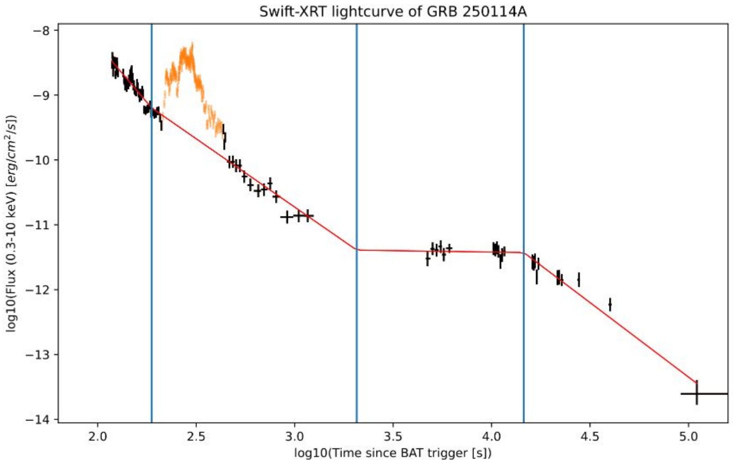

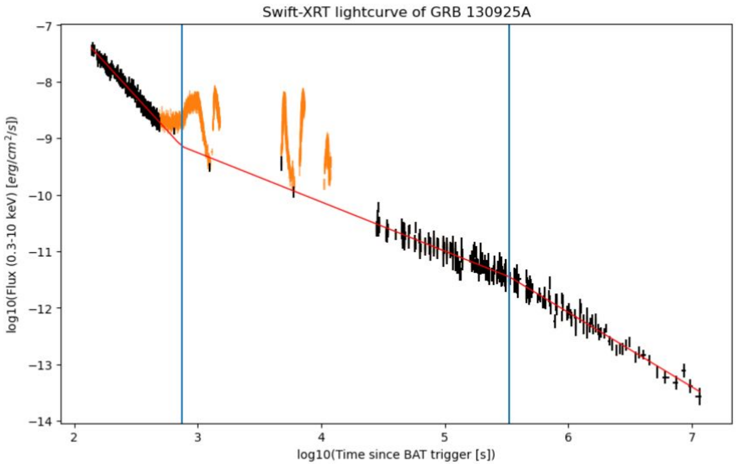

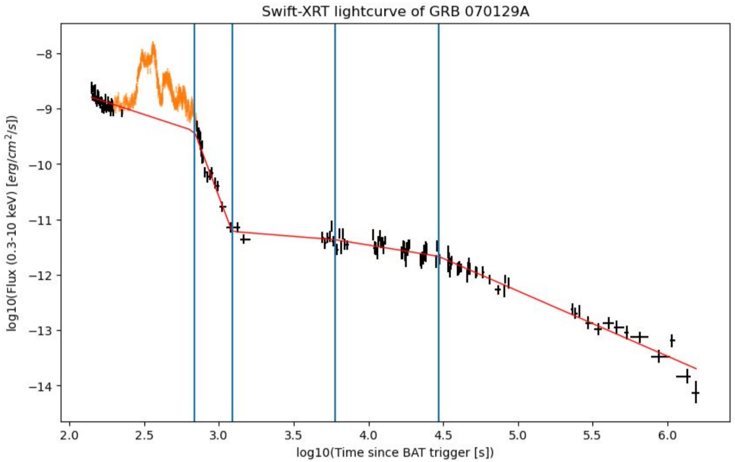

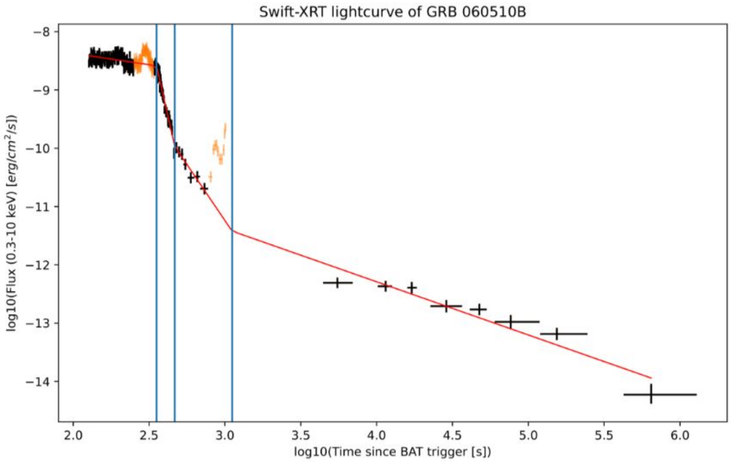

The raw data reproduce the claimed anti-correlation

In a raw comparison, 92 HE/VHE bursts appear less complex than 1123 non-HE bursts.

GRBs with HE detection: simpler X-ray lightcurves with fewer breaks.

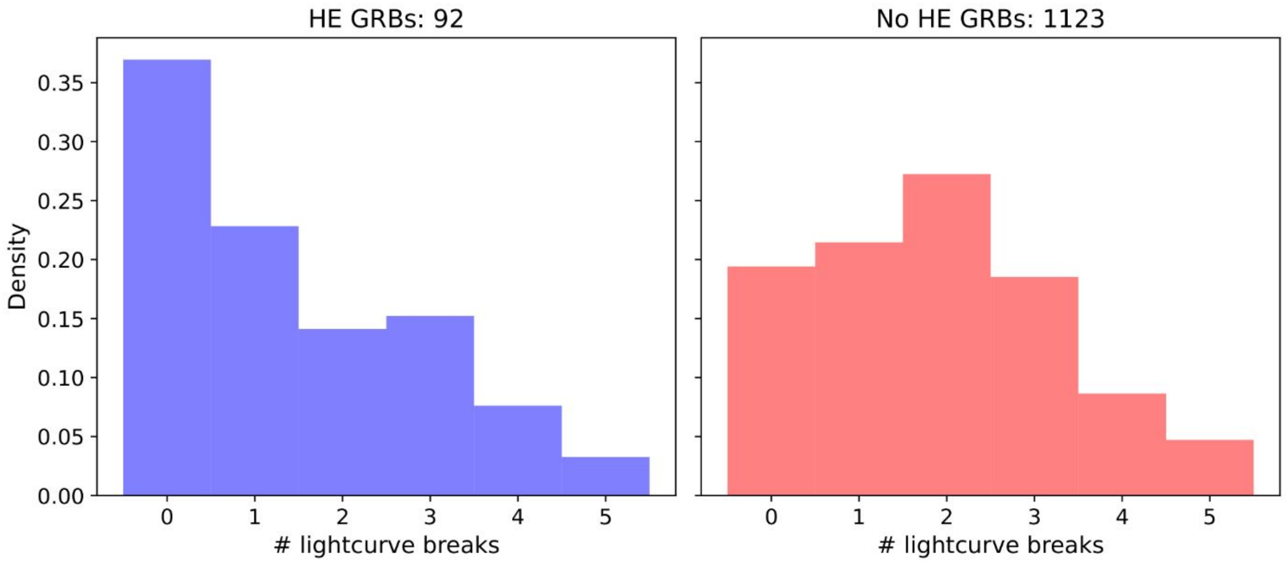

GRBs without a HE detection: broader complexity distribution for their X-ray lightcurves

Plateaus show the same raw pattern. At this point, earlier claims appear confirmed.

The role of the data-taking start time t_{XRT}

Observations starting later (high t_{XRT}) are less likely to capture early, complex features like breaks and plateaus.

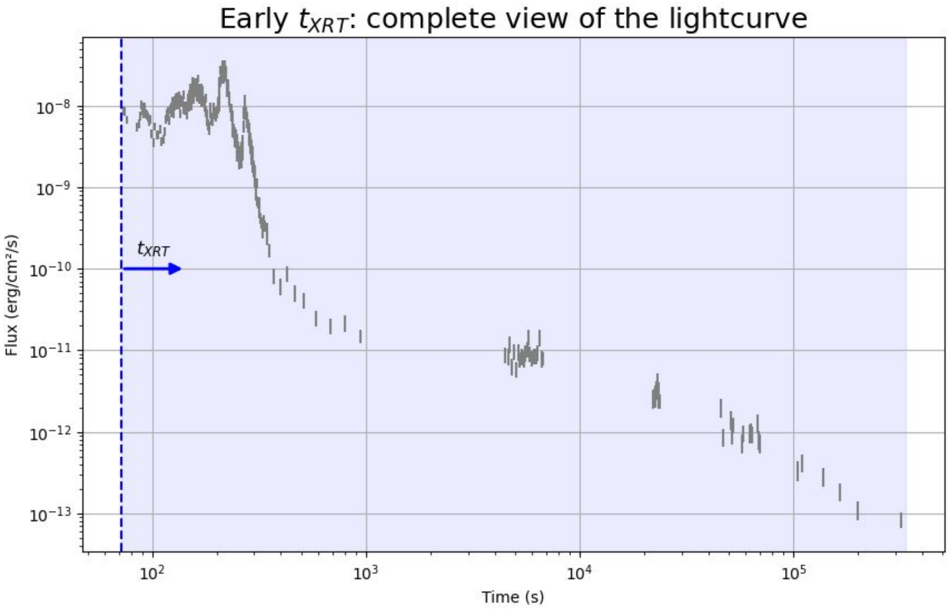

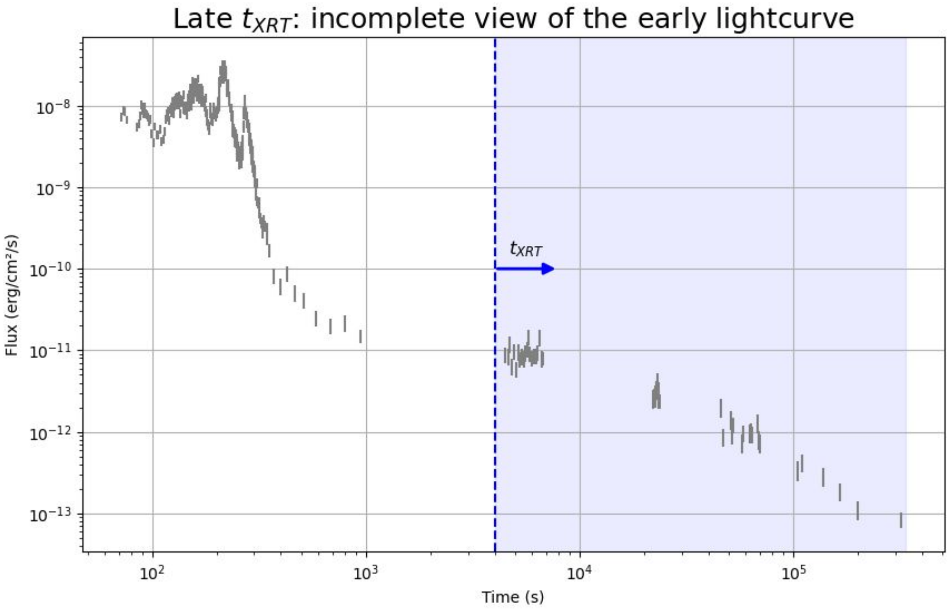

If HE and non-HE samples have different t_{XRT} distributions, their apparent morphology can differ even when the intrinsic populations do not.

Swift operations: t_{XRT} for GRBs with and without a HE detection

The distribution of Swift-XRT observation start times is not the same for GRBs with and without HE detections!

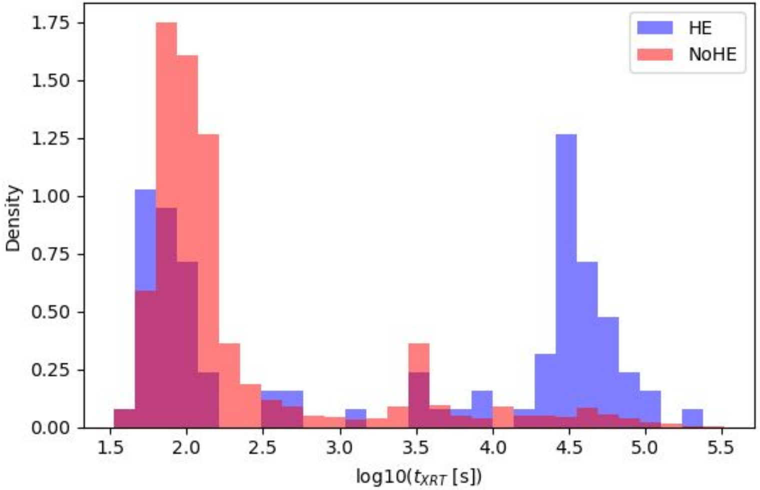

We are not comparing physically distinct samples, but observationally biased ones.

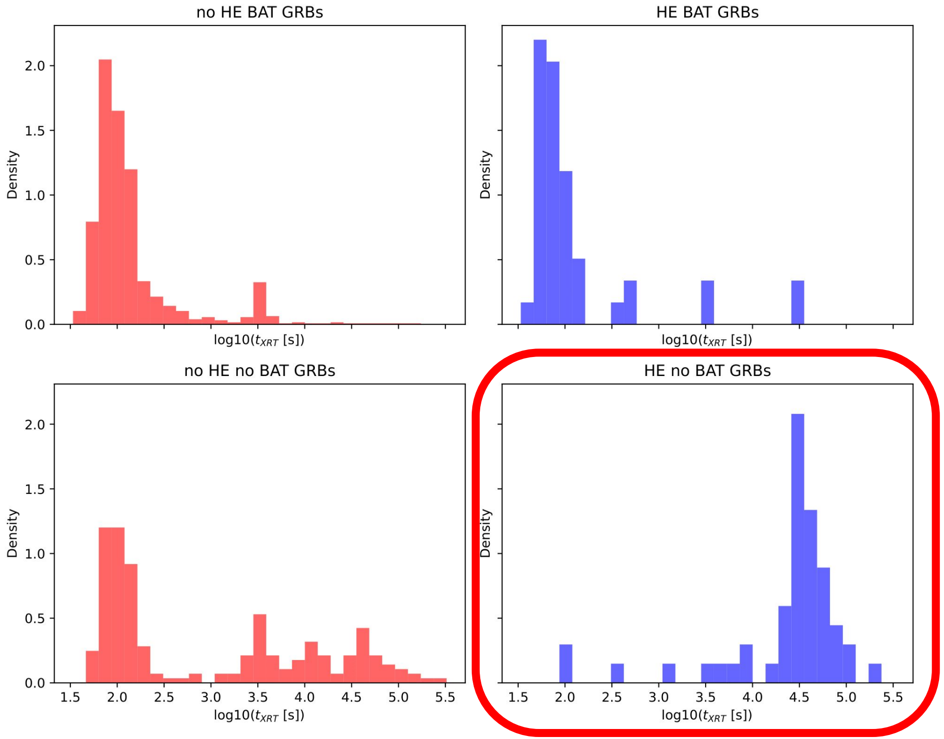

The HE sample is bimodal, with a late-start component at $t_{XRT} \geq 10^4$ s

When accounting for t_{XRT}, the complexity difference vanishes

We stratified the sample into four logarithmic t_{XRT} bins and repeated the comparison within each bin.

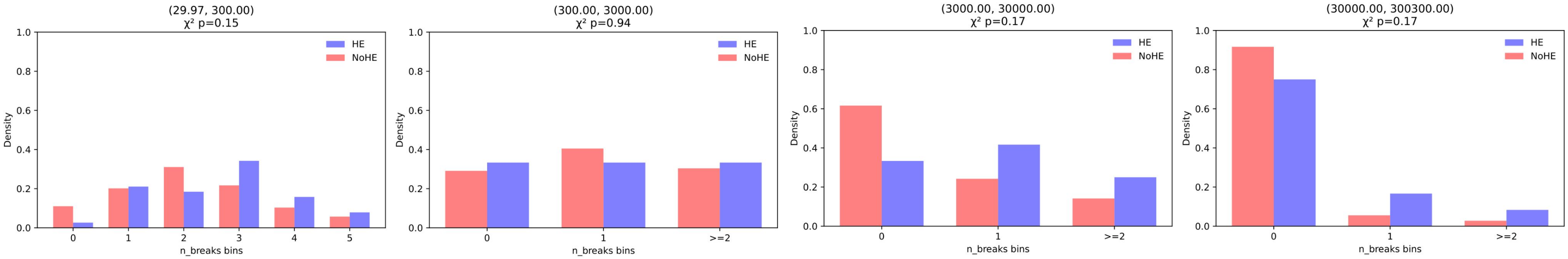

Within any given t_{XRT} bin, GRBs with HE emission are just as complex as those without.

Is t_{XRT} the true driver of complexity?

Using a Poisson Generalized Linear Model (GLM) we tested the predictive power of both t_{XRT} and HE detection on the number of lightcurve breakpoints.

$$\ln(\mathbb{E}[n_{\mathrm{breaks}}]) = \beta_0 + \beta_{\mathrm{HE}} \cdot \mathrm{HE} + \beta_{t_{XRT}} \cdot \log_{10}(t_{XRT}) + \beta_{\mathrm{int}} \cdot \mathrm{HE} \times \log_{10}(t_{XRT})$$

Coefficient	Estimate	Std. Error	$z = \frac{\text{Coefficient}}{\text{Std. Error}}$	p-value
β_0	2.29	0.109	21.09	< 0.0001
β_{HE}	−0.16	0.25	−0.67	0.5
$\beta_{t_{XRT}}$	−0.77	0.053	−14.46	< 0.0001
β_{int}	0.14	0.11	1.26	0.21
Model summary: Log-likelihood = −1871.4, Deviance = 1186.2, Pearson χ^2 = 1050, df = 1211, pseudo-R^2_{CS} = 0.28, overdispersion ratio = 0.87.				

After accounting for t_{XRT}, the presence of high-energy emission provides no additional predictive power for afterglow complexity.

The raw data also suggest fewer plateaus in HE GRBs

Before controlling for t_{XRT} plateaus appear less often in events with HE detections.
The duration distributions are not significantly different (KS p=0.67).

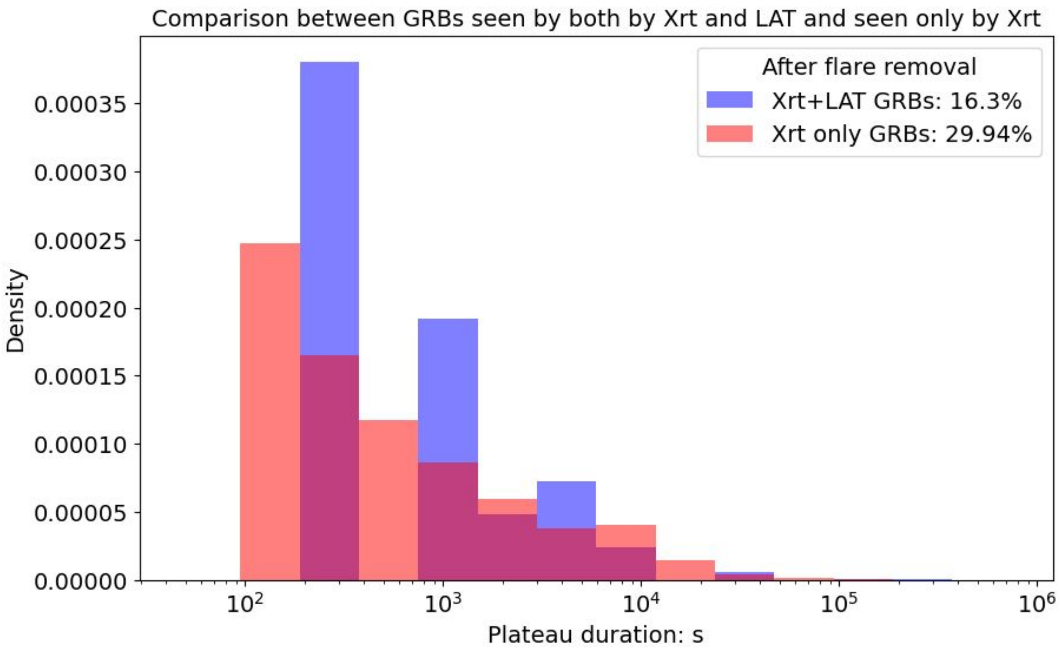

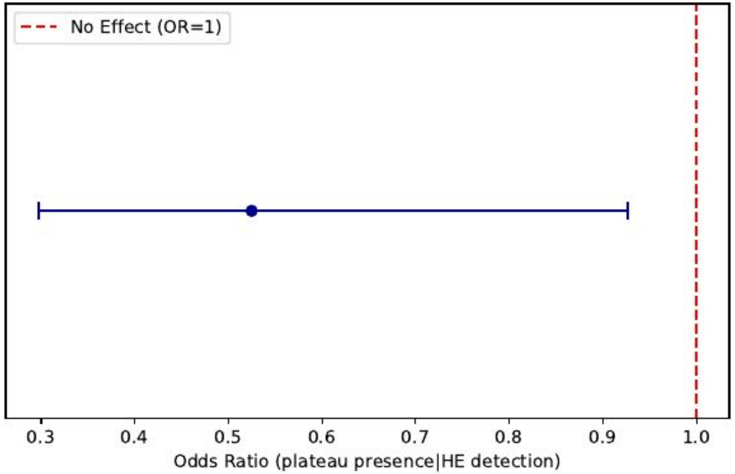

Odds ratio (OR) for the association between HE detection and plateau phases.
The vertical dashed red line marks no association.

The apparent plateau deficit also disappears with t_{XRT} controll

Stratified odds ratios are consistent with no association between HE detection and plateau incidence.

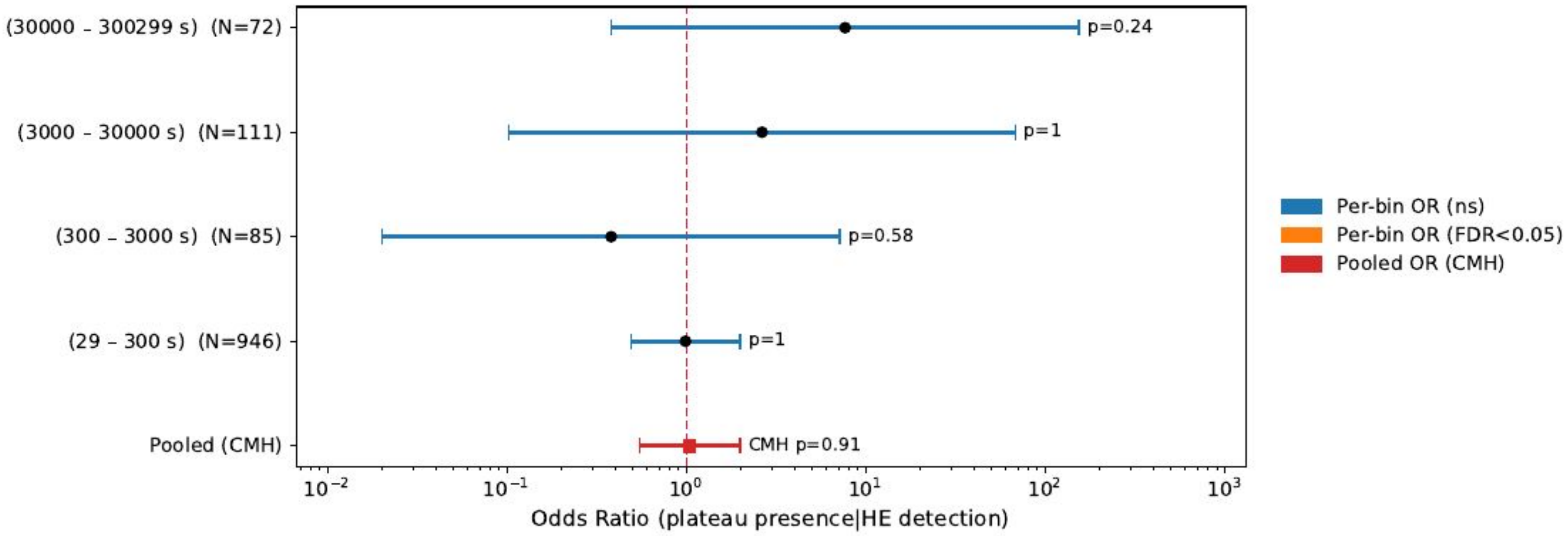

The pooled test remain non-significant once t_{XRT} is accounted for.

Not limited to breaks and plateaus: α_1

No statistically significant difference in the distributions of α_1 between GRBs with and without HE detections once t_{XRT} is accounted for.

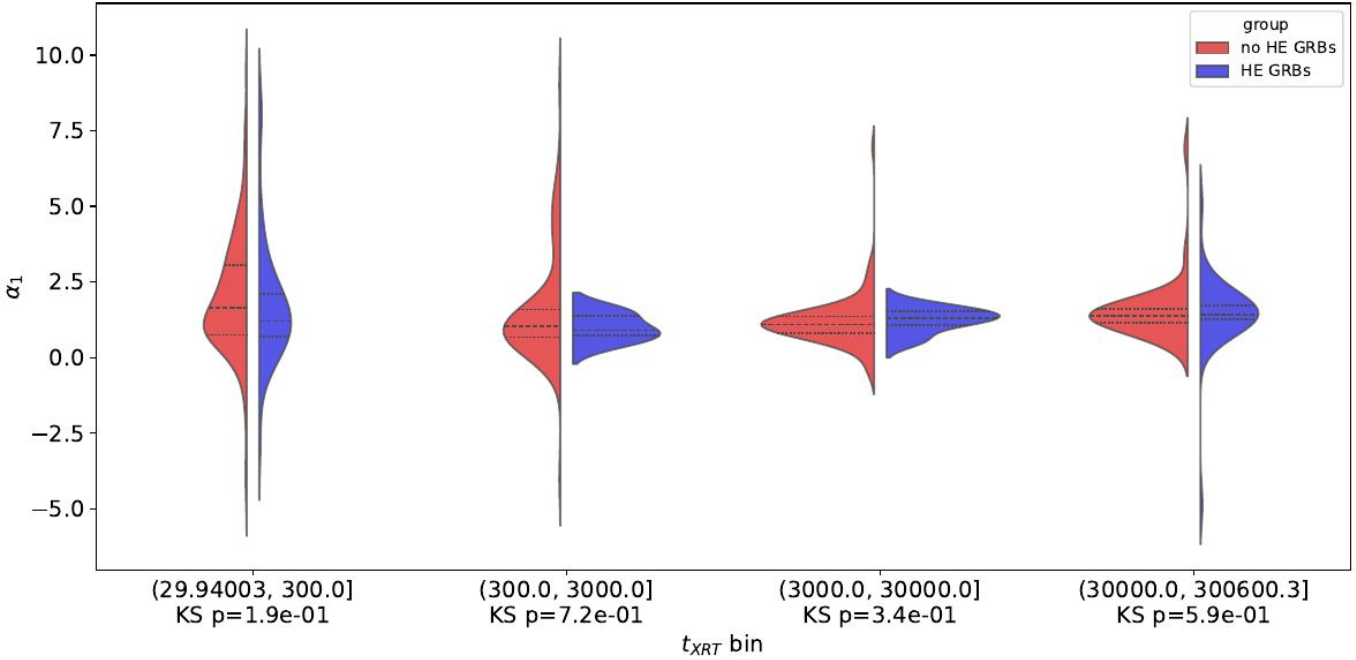

No link between HE and X-ray afterglow morphology

- Apparent correlations (complexity, plateaus, α_1) vanish once t_{XRT} is controlled
- Same conclusion from stratification, GLMs, and pooled tests
- HE and non-HE GRBs are statistically indistinguishable in XRT morphology

NB: not proof that every physical link is absent, but morphology is not a validated HE/VHE predictor.

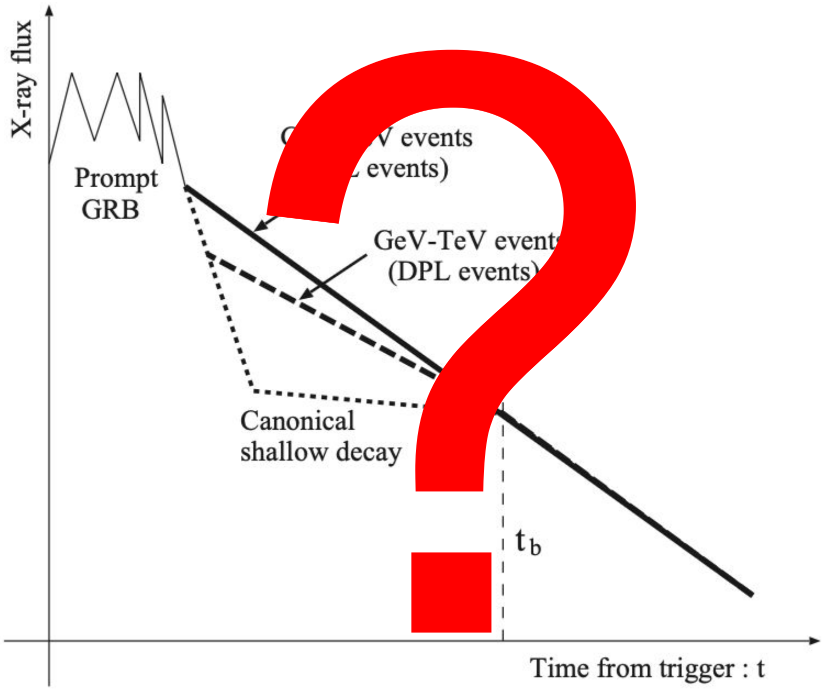

A cautionary tale for VHE observations

GRB 190114C: similar XRT–MAGIC decay

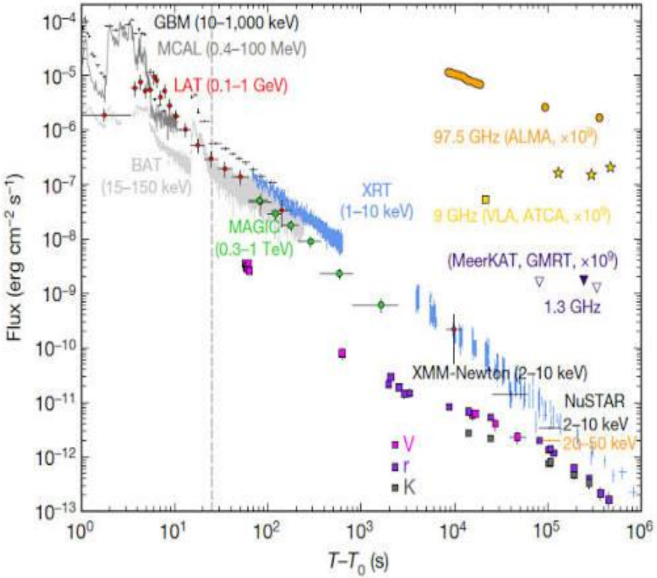

MAGIC Collaboration et al., Nature 575, 459–463 (2019)

Same intrinsic evolution

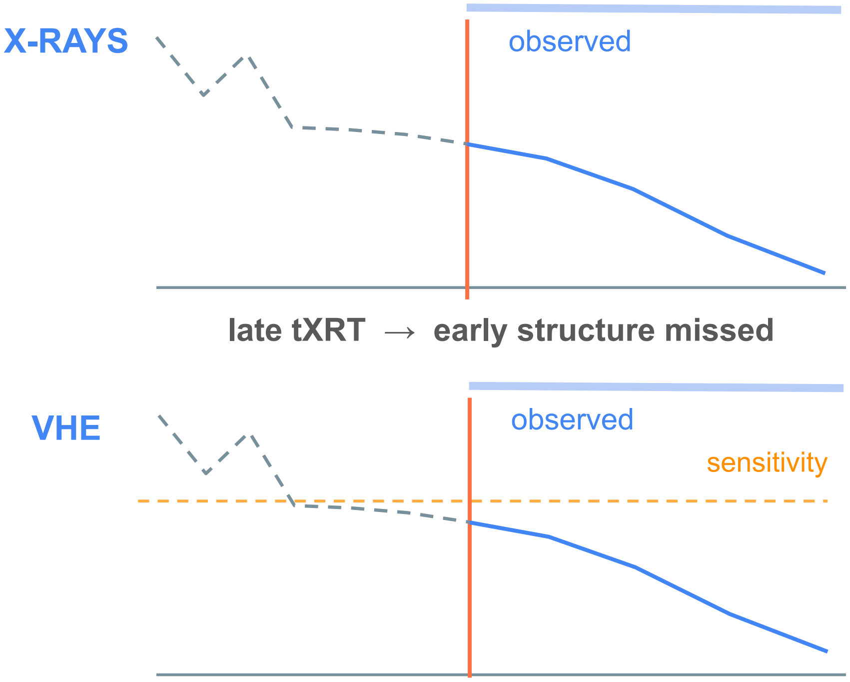

late tXRT → early structure missed

latency → the same emission is missed

Vigliano et al, 2026

Lessons learned

We developed a new tool to test correlations in GRBs in large samples.
From this analysis it appears:

- Large samples are fundamental to probe empirical correlations.
- Large samples do not automatically remove bias.
- Homogeneous analysis is necessary but not sufficient.
- Confounders must be modeled explicitly.
- Better observational programs are needed.

We must move on from single/few events analyses toward more statistically robust approaches

Backup

Summary & Conclusions

- GRB correlations connect prompt emission, afterglow morphology, high-energy emission and possible propagation physics.
- Their interpretation is limited by selection effects, instrumental thresholds, cadence and analysis choices.
- In the HE/XRT case study, apparent morphology correlations vanish once observational biases are controlled.

For the future:

- Biases must be considered in any analysis or they might lead to biased comparison and incorrect physical conclusions
- The field of GRB analysis must move on from the current strategy of analysing single bursts toward statistically solid large-sample analyses
- Better strategies for observation and subsequent analysis on large scales must be developed to tackle the large datasets expected from current and new missions such as SVOM, Einstein Probe and CTAO.

Observing strategies for rare high-energy transients

Strategy	What it improves	Relevance for GRB
Fast repointing	Reduces latency after GRB alerts	Catches rapidly fading HE/VHE emission

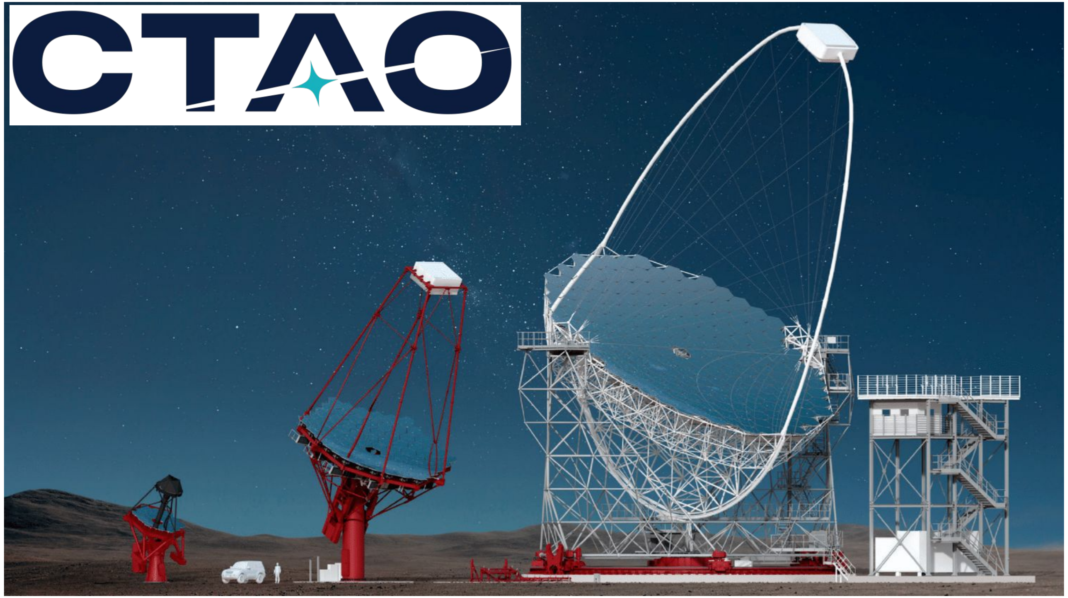

Observing strategies for rare high-energy transients

Strategy	What it improves	Relevance for GRB
Fast repointing	Reduces latency after GRB alerts	Catches rapidly fading HE/VHE emission
Tessellated follow-up	Covers large localization regions with multiple pointings	Useful for poorly localized GRBs, GW/neutrino counterparts

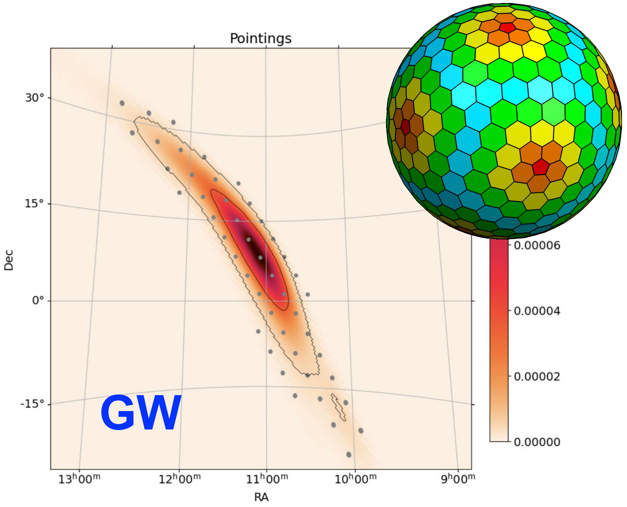

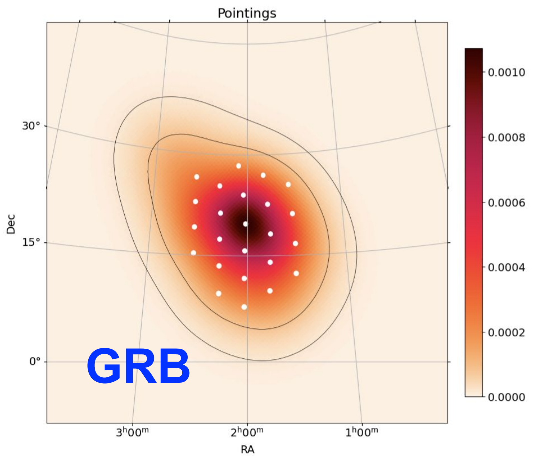

Observing strategies for rare high-energy transients

Strategy	What it improves	Relevance for GRB
Fast repointing	Reduces latency after GRB alerts	Catches rapidly fading HE/VHE emission
Tessellated follow-up	Covers large localization regions with multiple pointings	Useful for poorly localized GRBs, GW/neutrino counterparts
Divergent pointing	Increases instantaneous field of view	Trades some sensitivity/uniformity for higher transient coverage

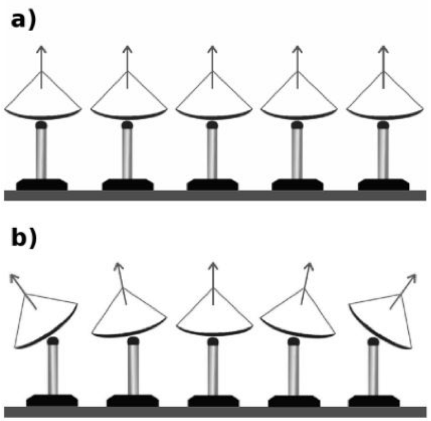

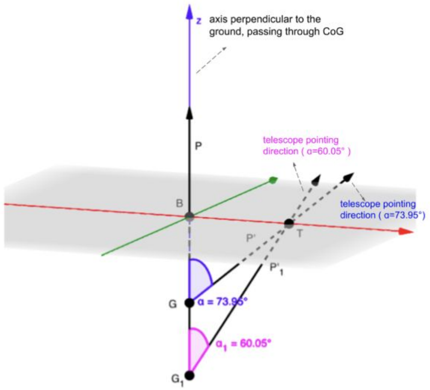

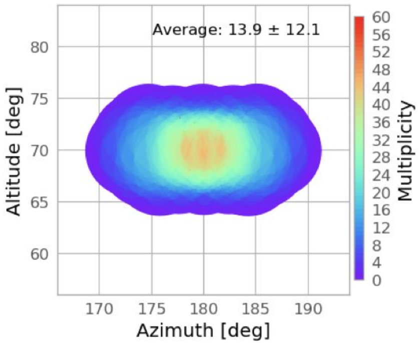

Observing strategies for rare high-energy transients

Strategy	What it improves	Relevance for GRB
Fast repointing	Reduces latency after GRB alerts	Catches rapidly fading HE/VHE emission
Tessellated follow-up	Covers large localization regions with multiple pointings	Useful for poorly localized GRBs, GW/neutrino counterparts
Divergent pointing	Increases instantaneous field of view	Trades some sensitivity/uniformity for higher transient coverage
Wide-field monitors	Continuous sky coverage	Provides early triggers and population context
Coordinated multi-instrument campaigns	Better temporal and spectral coverage	Reduces gaps between prompt, X-ray, GeV and TeV observations